

## The Enhancement of 3 MHz Ultrasonic Echo Signal for Conversion Curve Development for Acoustic Impedance Estimation by Using Wavelet Transform

Edo Bagus Prastika<sup>[1]</sup>, Agus Indra Gunawan<sup>[1]</sup>, Bima Sena Bayu Dewantara<sup>[1]</sup>, Chandra Edy Prianto<sup>[1]</sup>, Naohiro Hozumi<sup>[2]</sup>

Politeknik Elektronika Negeri Surabaya (PENS)<sup>[1]</sup>  
Surabaya, Indonesia

Toyohashi University of Technology<sup>[2]</sup>  
Toyohashi, Japan

prastikabagusedo@gmail.com, agus\_ig@pens.ac.id, bima@pens.ac.id,  
chandraedyp@gmail.com, hozumi@ee.tut.ac.jp

### Abstract

Ultrasonic technology has already been applied for many applications. Most of them are mainly used for object measurement. Some techniques have been widely applied to particular measurement by utilizing a very specific component. In this research, the previous technique to develop a conversion curve to obtain the acoustic impedance of the target is adopted. Then, a 3 MHz concave shaped ultrasonic transducer for measuring liquids is proposed and a confirmation is needed to confirm if the system is correct. Therefore, several saline solutions with some known properties are used. A low voltage of 10 Volt pulse is sent to trigger the transducer. The ultrasonic wave is transmitted through the multilayered mediums, which is pure water, clear acrylic, and the target. The echo from the interface between the acrylic and the target is then received by the same transducer. Some parameters such as peak and Root Mean Square (RMS) are used to develop the conversion curve. A peak detection and comparison between the original echo and the processed one by using Wavelet transform is performed. Some analysis of the echo signal by using multiresolution and time-frequency analysis are also proposed. The result obtained from the measurement is then compared to the theoretical calculation. Based on the result, in terms of developing the conversion curve, only the RMS value of the Undecimated Wavelet Transform (UWT) which has the closest trend to the result of the calculation, with the mean percentage error of 0.65512%, which is the smallest value among all parameters.

**Keywords:** Ultrasonic, Echo, Conversion Curve, Wavelet, Acoustic Impedance.

## 1. INTRODUCTION

In ultrasound measurement, one of the method to calculate the acoustic impedance value is by using a conversion curve, which converts the value of peak-to-peak or the Root Mean Square (RMS) of an echo signal into acoustic impedance [1-9]. However, the RMS and peak-to-peak value cannot be measured directly because sometimes the received echo signal is contained with noise which frequency is higher than the echo frequency. This noise will affect the amplitude and the shape of the signal, which will change the value of the peak-to-peak and RMS as well. In this research, the Wavelet transform is applied to overcome this problem, because Wavelet can remove the noise without losing the original profile of the signal [10-13], compared to the conventional Bandpass filter method. The Wavelet transform can also be applied to detect the peak of the signal more precisely, compared to the conventional peak detection such as curve fitting method. There are previously some researches which applied the Wavelet method in Ultrasonic field [14-16]. An analysis in time-frequency domain is also performed with the Scalogram as the output, to observe the parameters of the signal such as time, frequency, and the amplitude as the signal propagates through the medium. The output of the research will be the normalization graph of the RMS and peak-to-peak of the echo signal as the basis of the development of the conversion curve.

## 2. RELATED WORKS

The research about the application of the Wavelet transform has been applied in many fields of study, such as ultrasound and biomedical field [12-13][17-19] because Wavelet can maintain the detail of the original signal as well as removing the unused part such as noise and reconstruct the signal [20]. In the previous research about developing a conversion curve from an echo signal [12-15], the method to remove the noise of the signal is not discussed in detail, it is either because the echo signal can instantly be processed or because the need for signal pre-processing is not necessary. However, in some cases [14-16], a pre-processing is required for the echo signal in order to obtain the best quality of the signal parameters applied for developing a conversion curve.

## 3. ORIGINALITY

The contribution of this series of study is to implement the Wavelet transform for denoising and perform a better detection of the received echo signal in order to obtain the best parameters to develop a conversion curve required for acoustic impedance estimation. Because in the previous research which also developed a conversion curve from the echo signal [1-9], the pre-processing method of the echo signal was not discussed in detail. It is either because the profile of the received echo signal was already good or because a pre-processing of the signal is not required. However, in practice, the received echo signal does not always meet the requirement so a pre-

processing method is needed. In this research, the result of the echo signal processing by using Wavelet transform is compared to the conventional filtering method such as a Bandpass filter. A better peak detection and some analysis such as time-frequency analysis of the echo parameters while propagating into several multilayered mediums, and a multiresolution analysis are also performed.

**4. SYSTEM DESIGN**

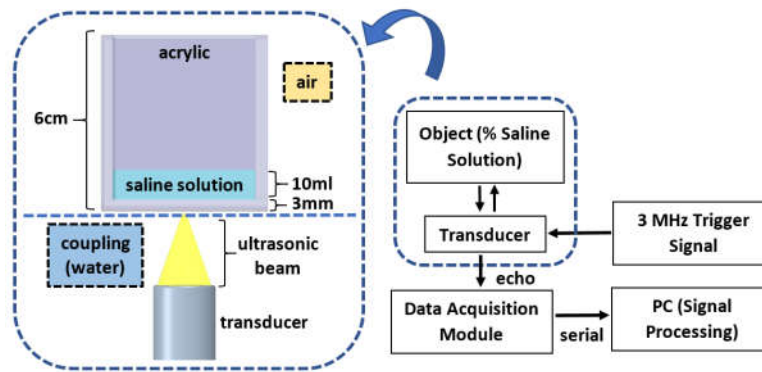


**Figure 1.** Illustration for the detailed setup of the target.

The design of the system in this research is shown in Figure 1. A 3 MHz trigger signal is sent to the transducer by a signal generator (GW Instek GFG-3015). The transducer is a 3 MHz immersion probe transceiver (ISP5-10-20) which has a focused beam with the focal length of 20 mm. The transducer transmits an ultrasonic wave that propagates through the multi-layered mediums. The reflected echo from the target is received by the same transducer and acquired by a data acquisition module (Agilent Technologies InfiniVision MSO6054 500 MHz).

As the target, several saline solutions with a different level of weight percentage that varies from 0 – 10% with the increment of 2% is used. In order to keep the target from being contaminated, a clear acrylic (acoustic impedance  $Z = 3.26 \text{ MNS/m}^3$ , density  $\rho = 1185 \text{ kg/m}^3$ , speed of sound  $c = 2730 \text{ m/s}$ ) with the thickness of 3 mm is chosen to separate target and coupling water.

**4.1. THE WAVELET TRANSFORM FOR ULTRASONIC SIGNAL DENOISING**

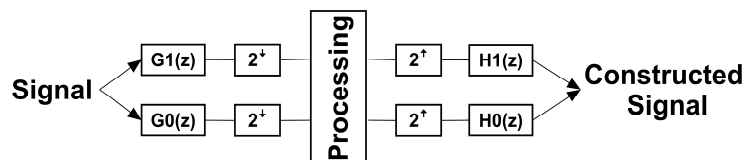


**Figure 2.** Filter banks with two channels perfect reconstruction (PR)

There are two methods of denoising performed in this research, that is by using the Discrete Wavelet transform (DWT) and the Undecimated Wavelet transform (UWT). In order to apply the DWT method, the discrete filter banks are required to calculate the discrete Wavelet coefficients, the most efficient method is by using the filter banks with two-channel perfect reconstruction (PR), as shown in Figure 2. The input signal  $X[z]$  is filtered by the filter banks that consists of  $G_0(z)$  and  $G_1(z)$ , and downsampled by the number of 2 [13] :

$$y_{low}[n] = \sum_{k=-\infty}^{\infty} x(k)g(2n-k)$$

$$y_{high}[n] = \sum_{k=-\infty}^{\infty} x(k)h(2n+1-k) \tag{1}$$

After the processing stage, the upsampling is done with the factor of 2 on the modified signal and will be re-filtered by using the other filter banks that consists of  $H_0(z)$  and  $H_1(z)$ . The two-channel of PR filter banks can be applied and respectively split the output of the lowpass filter, as shown in Figure 3.

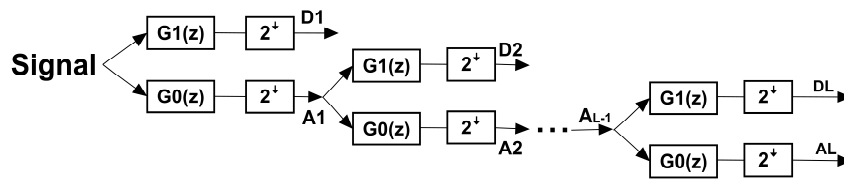


**Figure 3.** The discrete Wavelet transform

The A and D symbol stand for approximation and detail of the signal. The signal and the coefficients of DWT can also be constructed by using the inverse DWT, as shown in Figure 4.

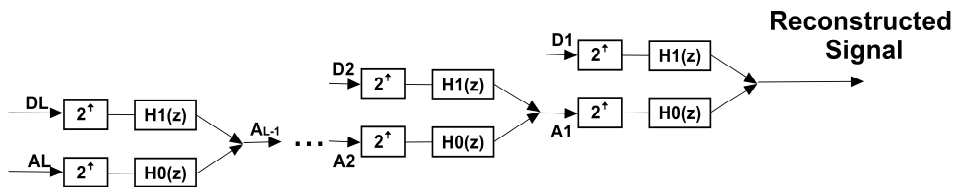


**Figure 4.** The inverse discrete Wavelet transform

In the previous research about power quality detection by using multiresolution Wavelet [21], DWT provides enough information and at the same time is more efficient in terms of computational time. Unlike DWT, UWT does not require a downsampling operation, which means that the original signal will have the same length as the approximation and the detail coefficients on each level [20]. The multilevel decomposition of the UWT concept is shown in Figure 5. By comparing UWT and DWT, then UWT has some good features, such as the capability of performing a better signal

denoising, and also the capability of detecting the peak of a signal which is better than DWT [20].

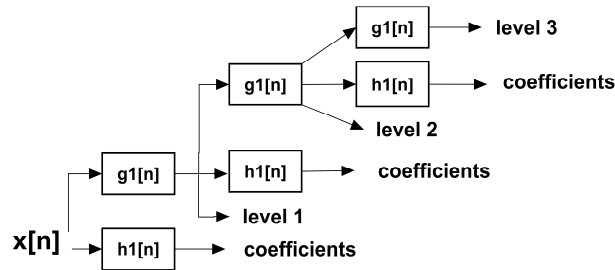


**Figure 5.** The multilevel decomposition of UDWT

The result of the peak detection by using UWT and DWT will be compared with the curve fitting method, which is normally applied for R detection of an Electrocardiograph (ECG) signal [22-23]. The Wavelet transform can decompose the components of a signal that is overlapped to each other [19][21]. On the multiresolution analysis (MRA), the Wavelet and the scale function are applied as the parts to split and reconstruct a signal into some levels with different resolution. The detail part of the decomposed signal will be generated by the Wavelet function, and the approximation will be generated by the scale function. Mathematically, it can be represented as [21] :

$$f(t) = \sum_k c_0(k) \Phi(t-k) + \sum_k \sum_{j=0}^{j-1} d_j(k) 2^{\frac{j}{2}} \Psi(2^j t - k) \tag{2}$$

Where  $c_0$  is the coefficient of scale level at '0' and  $d_j$  is the Wavelet coefficients on the scale of j.  $\Phi(t)$  and  $\Psi(t)$  respectively are the scale function and the Wavelet transformation, and  $k$  is the translation coefficient.

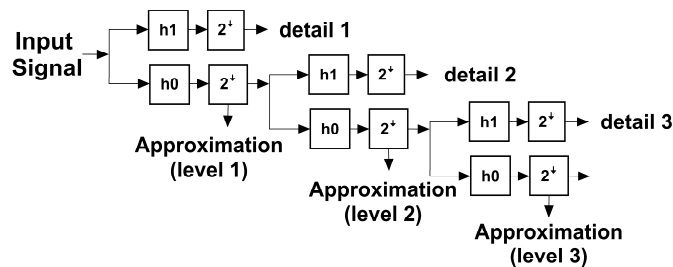


**Figure 6.** The signal decomposition with a three-level of multiresolution

Figure 6 shows a scheme of three-level multiresolution signal decomposition. If the level is increased, we will get the approximation and detail of the signal with a larger scale.

## 5. EXPERIMENT AND ANALYSIS

As shown in Figure 7, there are three signals received by the transducer, they are  $S_0$ ,  $S_1$ , and  $S_2$ . Where  $S_0$  is the signal received from the first interface between the coupling medium (water) and acrylic,  $S_1$  is the signal received from the interface between the acrylic and the target (saline solutions), and  $S_2$  is the signal received from the interface between the target and the air outside.

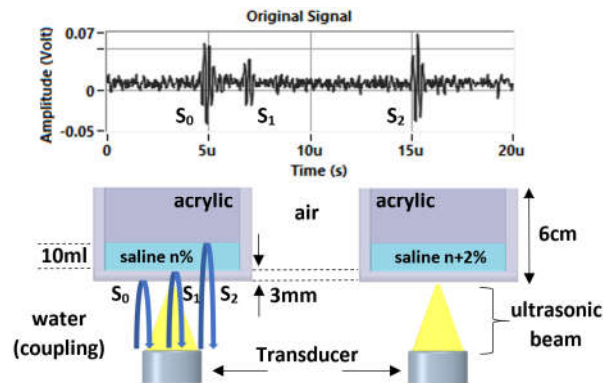


**Figure 7.** The echo received from each layer of the target

The observation will focus on  $S_1$ , which is the signal that has a direct contact with the target being measured.

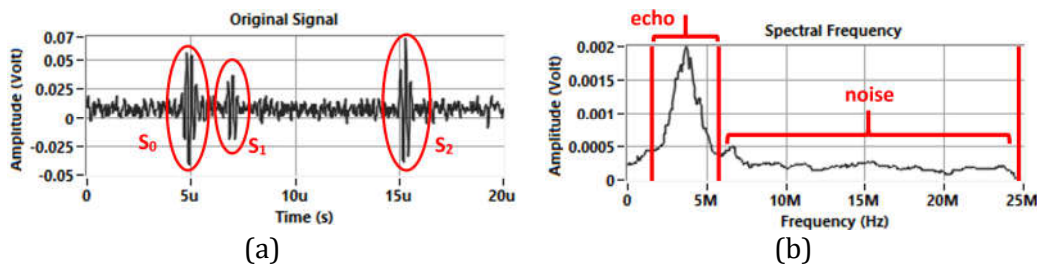


**Figure 8.** The received echo signal and its spectral measurement

Figure 8(a) shows the received echo signal with the target measured is 2% of saline solution with the weight percentage of 2% and Figure 8(b) shows its spectral measurement calculated by using Fast Fourier Transform (FFT). On the result of its spectral measurement, the noise which frequency is higher than the trigger frequency (3 MHz) is until the frequency of 25 MHz. The frequency distribution of the three echo signals ( $S_0$ ,  $S_1$ , and  $S_2$ ) is from 3 MHz until less than 5 MHz. On the received echo signals, the distance between  $S_0$  and  $S_1$  is 2.13  $\mu$ s, as shown in Figure 9. With the speed of sound in the substrate (acrylic) that is 2750 m/s, the thickness of the acrylic used in the experiment can be calculated.

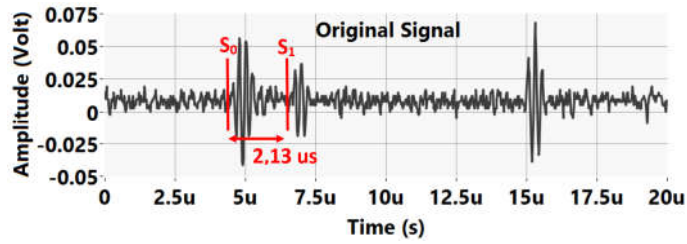


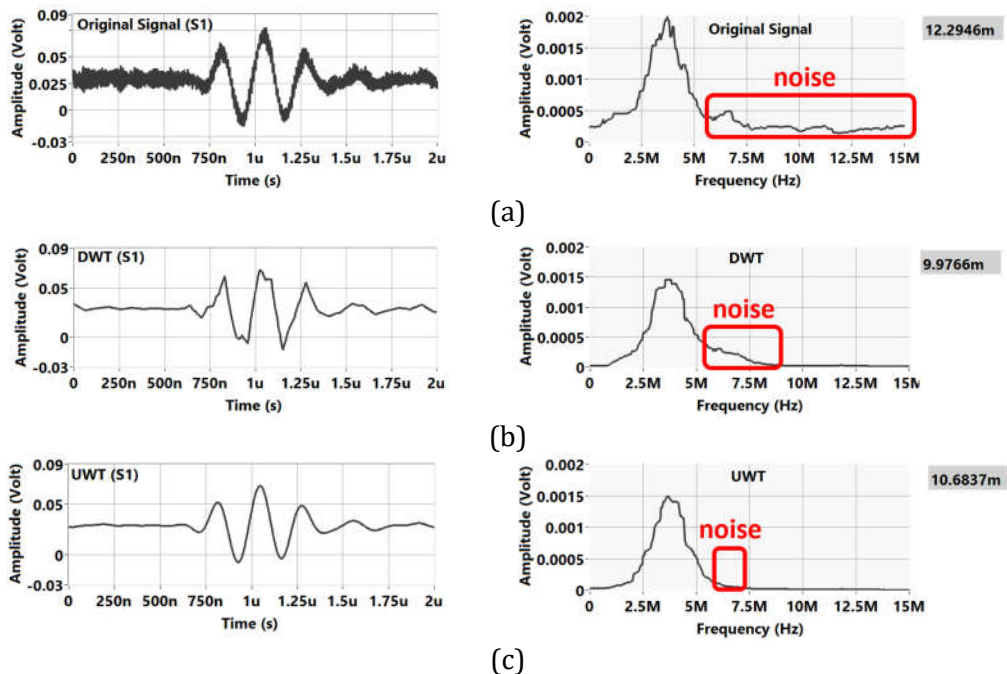
**Figure 9.** The distance between  $S_0$  and  $S_1$  in us.

So the travel time of the wave when propagates through the first and second medium ( $S_0$  and  $S_1$ ) can be calculated as follows:

The speed of sound in acrylic	= 2750 m/s
The distance between $S_0$ and $S_1$ ( $\Delta T$ )	= 2.13 us
The thickness of the acrylic	= $2750 \text{ m/s} * 2.13 \times 10^{-6} \text{ s}$
	= $5.85 \times 10^{-1} \text{ cm}$
	= 5.85 mm

Because the received echo travels twice (transmitted and received), the value above is divided by the factor of 2, thus the thickness of the acrylic based on the  $S_0$  and  $S_1$  signals is  $5.85 / 2 = 2.925 \text{ mm}$  (the value corresponds to the thickness of the acrylic used, which is 3 mm).

### 5.1. THE DENOISING OF THE ECHO SIGNAL BY USING WAVELET TRANSFORM



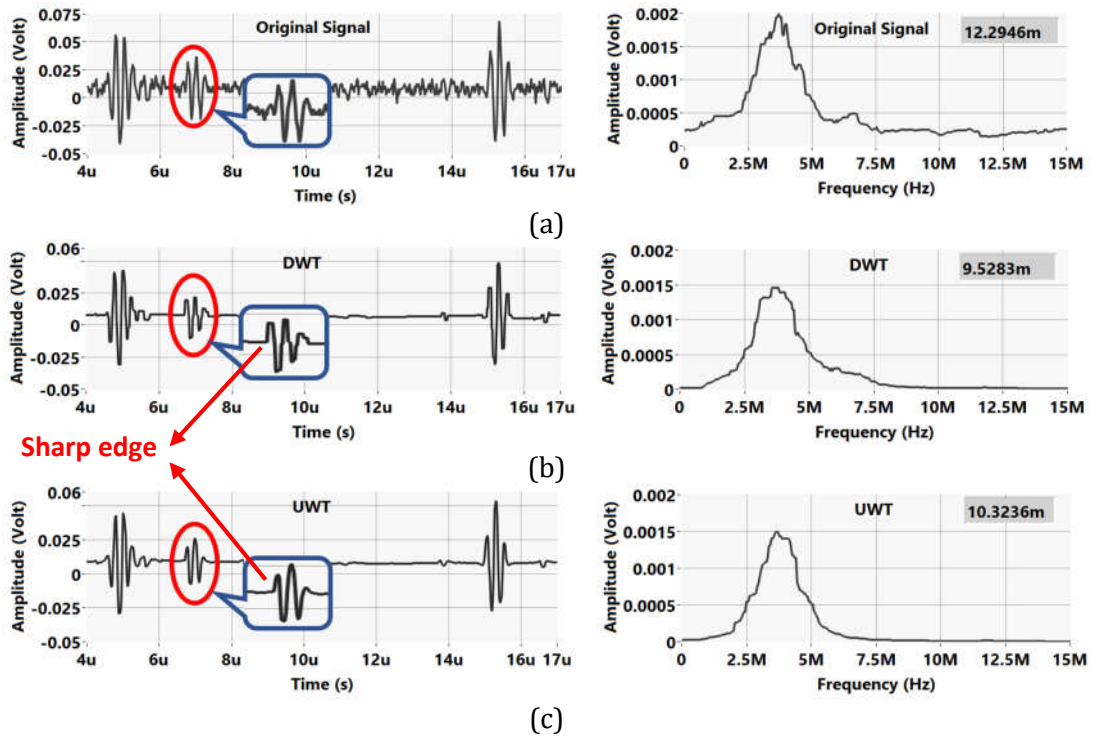
**Figure 10.** The result of denoising process and the spectral measurement by using the db13 Wavelet

Figure 10 shows the result of the denoising process (zoomed and stretched at the S1 signal) of 4% saline solution. The threshold for the approximation and detail coefficients for both UWT and DWT is set to  $\sqrt{2x \log(Ls)}$ , where  $Ls$  is the length of the signal, with the assumption that the noise is white, and then rescaling the threshold by using the variance of the noise. The sampling rate of the acquired signal is 10 nanoseconds. The RMS and the spectral measurement of the entire signal length of each filter are also calculated. Figure 10(a) is the original signal with the noise on it. As shown by its spectral frequency, the frequency of the noise almost covers all the signal frequency, even above the frequency of 10 MHz, and the main frequency is on the frequency of around 3 MHz until less than 5 MHz. On Figure 10(b), the denoising is carried out by the DWT, although the noise is quite reduced, there is still noise left on the frequency of around 11 MHz. Figure 10(c), is the denoising process conducted by the UWT, where the noise is more reduced until the frequency of below 7.5 MHz. Unlike the DWT method, the RMS value of the UWT is close to the original signal, it is because the UWT method can maintain the profile of the original signal, compared to the DWT method. The DWT method is actually more efficient in terms of computation than the UWT method. However, it is difficult to obtain the smoothness and accuracy at the same time when using the DWT, and also from the result above, the DWT method does not produce a smooth result of denoising, such as the UWT method does.

## 5.2. THE RELATION BETWEEN THE TYPE OF WAVELET AND THE SHAPE OF THE SIGNAL RESULT

The parameters chosen in the denoising process by using the UWT and DWT is the same, where the type of the Wavelet is orthogonal Wavelet with the type of Daubechies with the level of 13 (db13). This type of Wavelet is chosen because based on the result of applying the other type of Wavelets, even though they are capable to remove the noise, but they will result in significant changes on the signal shape, which is different from the original signal.

As shown in Figure 11, the Wavelet type of Haar with the level of 6 is used as a comparison to the db13 Wavelet. There are significant results between the Haar and the db13 Wavelet. The Haar Wavelet produces the output signal that is different from the original one. As shown in the figure, there are sharp edges on the resulted signal, either on the DWT (Figure 11(b)) and UWT (Figure 11(c)). Although in terms of functionality, as shown on its spectral measurement, the Haar Wavelet can also remove the noise on the higher frequency, as well as db13 Wavelet.



**Figure 11.** The result of denoising by using DWT and UWT with the wavelet type of Haar (level 6)

**5.3. THE COMPARISON BETWEEN UWT AND DWT METHOD**

By comparing the result of the UWT and DWT Wavelet, the UWT Wavelet visually has the same profile and shape as the original signal, as shown in Figure 10, the RMS value of both methods are different, where the RMS value of the original signal is 12.2946 mV. This value means the total RMS value of the signal and the noise on it. The DWT method has RMS value of 9.9766 mV and the UWT method has the RMS value of 10.6837, where based on the result of the signal and these RMS value, the RMS value of UWT method is quite close to the RMS value of the original signal. By focusing on the output signal between the acrylic and the target ( $S_1$  signal), the comparison of the signals are shown in Figure 12.

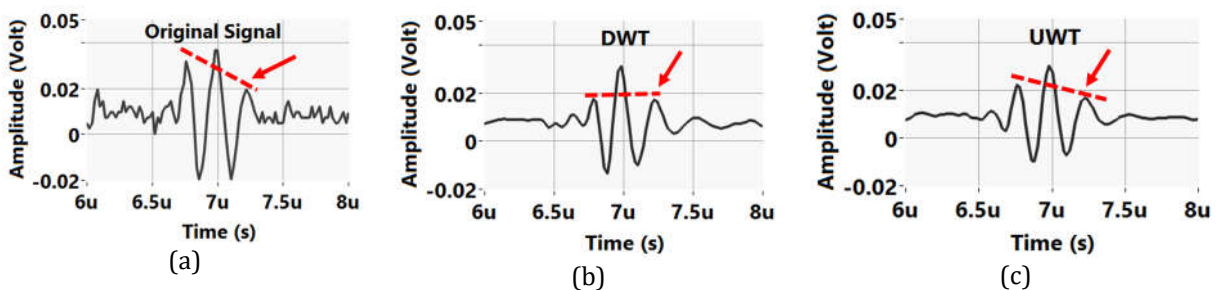


**Figure 12.** The comparison of the signal profile of the original signal, DWT and UWT of  $S_1$  signal

As shown in Figure 12, the comparison is focused on the area pointed by the red arrow. Figure 12(a) is the original signal, where the pointed area is lower than the two areas on its left. In the result of DWT (Figure 12(b)), the pointed area has a similar length to the first area on its left, which means that the DWT method tends to change the profile of the original signal. This problem is solved by using the UWT method (Figure 12(c)), where the pointed area is lower than the two areas on its left. The resulting signal of UWT method also has a lot of similarities to the original signal.

#### 5.4. THE COMPARISON BETWEEN WAVELET METHOD AND THE CONVENTIONAL BANDPASS FILTER

As a comparison, the result of the denoising process by using Wavelet is compared with the result of a conventional filter. In this research, the second order of a Bandpass filter is chosen.

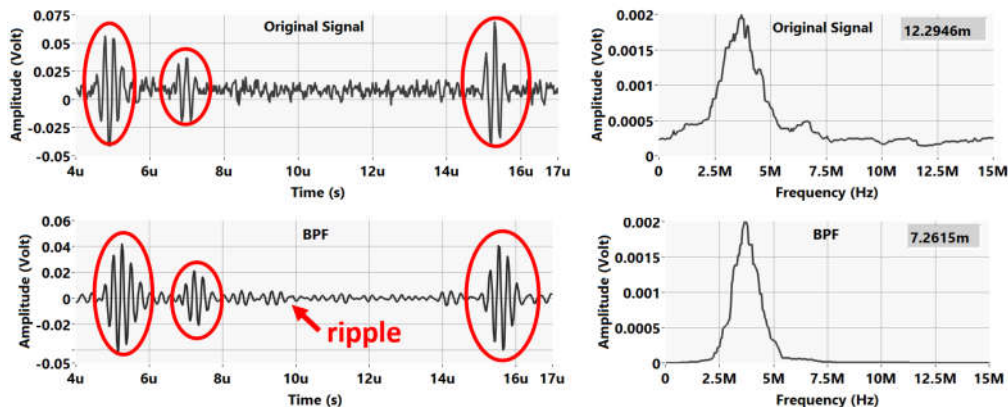


**Figure 13.** The comparison of the result of the Wavelet method and the conventional (bandpass) filter method

The result is shown in Figure 13, a Bandpass filter with the low frequency of 2.5 MHz and the high frequency of 5 MHz is chosen. The output of the Bandpass causes the change of almost the entire profile of the signal. From the RMS value and the result of the spectral measurement, the RMS value of the Bandpass filter has the smallest value among all, that is 7,2615m (DWT = 9.9766m, UWT = 10.6837m), this is actually related to the setting value of the cut-off frequency. Although on the spectral measurement, the output of the Bandpass filter can really suppress the frequency in the range of the cut-off limit. However, from the profile of the signal result, as shown by the arrow, the denoising process by using the Bandpass filter is less effective because the original profile of the signal is also changed, and in addition, there is still ripple on the resulted signal.

#### 5.5. PEAK DETECTION BY USING WAVELET TRANSFORM

The result of peak detection by using Wavelet compared to curve fitting method is shown in Figure 15, where the Wavelet method can locate the peak of the echo signal more precisely than the curve fitting method. The peak-to-

peak value of the Wavelet method is 47.2802, and the peak-to-peak value of the curve fitting method is smaller, that is 42.8002. The smaller value means that the gap between the two points of peak and valley is short, as shown in the figure, the gap between the green (peak) and the dark blue (valley) dots is shorter than the gap between the red and the blue dots (Wavelet method).

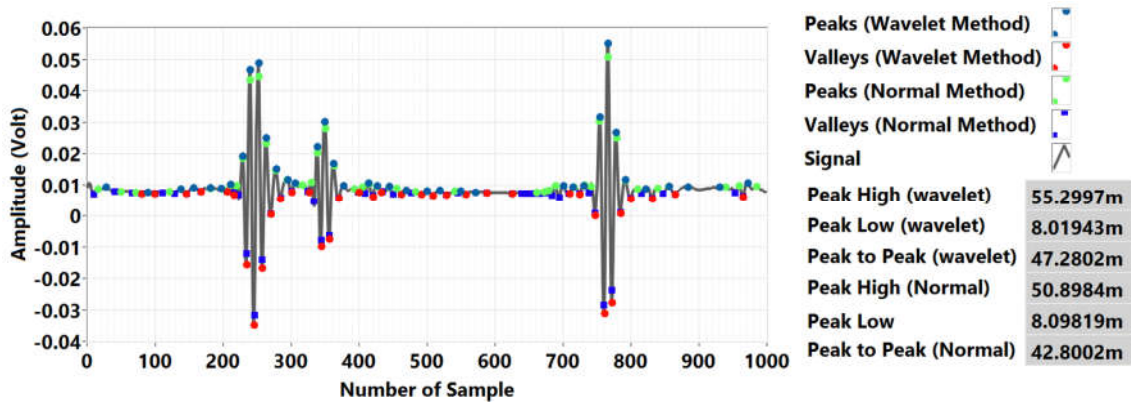


**Figure 14.** The comparison of the result of peak detection by using Wavelet and curve fitting method

### 5.6. MULTIREOLUTION ANALYSIS OF THE ECHO SIGNAL BY USING WAVELET TRANSFORM

The Wavelet transform can also be applied to perform a multiresolution analysis on a signal. This method can help us to understand more about a signal and the components that exist in it. Moreover, this method can also be applied to remove the unwanted component which is not needed in a signal, like noise.

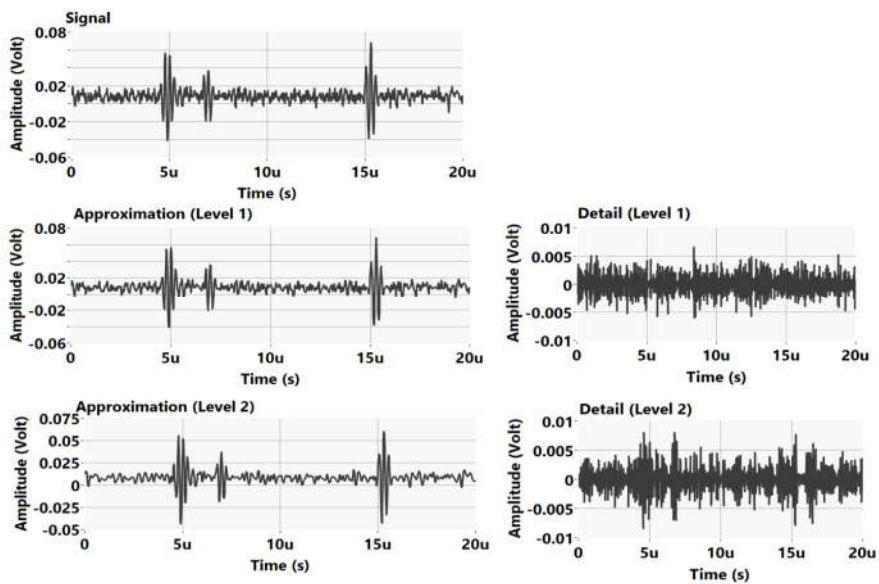


**Figure 15.** The multiresolution of echo signal by using Wavelet transform

This method basically splits a signal into two parts, a low and a high frequency components, where the low frequency mainly contains the information of a signal. This method can also be applied to the noised echo signal since the noise has a higher frequency than the original signal. The result of the application of this method is shown in Figure 15, the process splits the signal into two parts, its approximation which contains the low frequency and its detail which contains the high frequency. The number of the splitting process determines the level of the multiresolution analysis. The approximation at level 1 is basically the summation between the approximation 2 and the detail 2. The approximation at level 2 is the summation between the approximation 3 and detail 3. As the number of level increases, the approximation which contains the low frequency of the echo signal also gets smoother. Some signal processing can actually be performed here (at second approximation), after removing the high unwanted frequency of the signal. However, if the level is raised, the resulted signal is no longer smooth and the profile is unrecognizable, as shown in Figure 16.

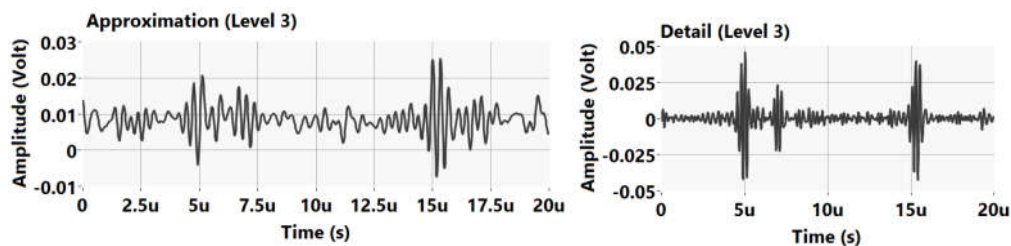


**Figure 16.** The third level of multiresolution analysis of the echo signal

As the level is raised, the resulted signal, especially on the approximation is no longer recognizable. It is because the resulted signal in the approximation 2 already has a low frequency, if the splitting process of the signal into its lower frequency is continued, the resulted signal will similar to the approximation 3, which no longer has the profile of the original signal, as shown in Figure 16. The profile of the detail 3, however, has more similarity to the original signal, it is because the signal in the detail 3 is the main signal of the echo (with a little noise on it). The spectral measurement of each result is shown in Figure 17.

In Figure 17, the detail of each level has a different frequency. On the detail 1, the frequency separated is at around 10 MHz – 25 MHz. The frequency separated on the detail 2 has a lower value, which is 5 MHz – 15 MHz. On the detail 3, the frequency separated is getting lower, which is around 3 MHz until 10 MHz. In terms of the amplitude of each detail, the amplitude of detail 1 and detail 2 is below 0.0005 Volt. The signal with the amplitude below 0.0005 Volt is the noise, which also covers the higher frequency. While the amplitude on the detail 3, however, is mixed between the amplitude of the original signal and the amplitude of the noise.

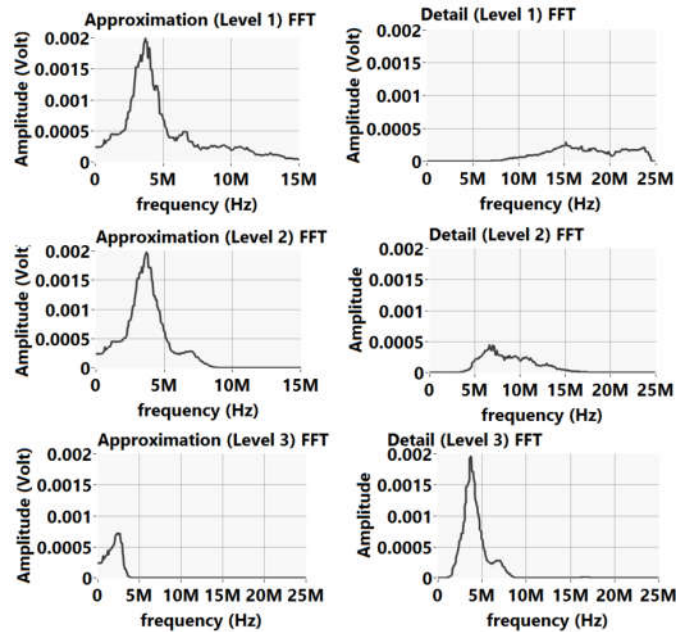


**Figure 17.** The spectral measurements of the multiresolution analysis

If the spectral measurement of the approximation and the detail at level 3 is zoomed in, the result is shown in Figure 18.

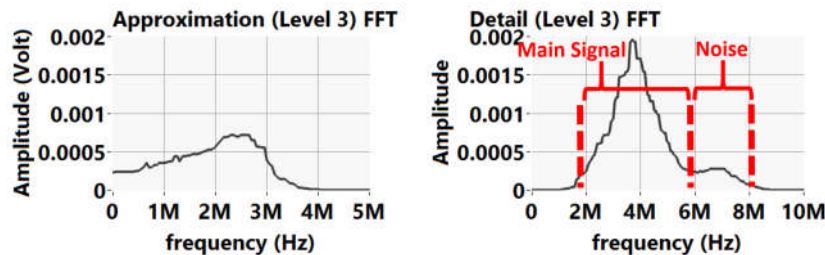


**Figure 18.** The spectral measurement on the approximation and detail 3 (zoomed in)

The signal in the detail 3 is a mixture between the signal with low frequency and the signal with high frequency. As shown by the red dotted line above, the signal which frequency is around 5.5 MHz – 8 MHz and the amplitude is below 0.0005 Volt is the noise, because, on the resulted echo signal in the time domain, the noise has a low amplitude and a high frequency. Where the signal below the frequency of 2.5 MHz – 5.5 MHz which the amplitude is above 0.0005 Volt is the main echo signal. As shown in the approximation result, the distribution of the frequency varies from 0 to less than 3.5 MHz. The distribution of the amplitude also varies from 0 to less than 0.0008 Volt. Based on this result, the signal in approximation 3 actually contains information about the original signal, but not much. Because in the process of the multiresolution analysis, the level taken in the process should be stopped at the second level (level 2). However, since the process is

continued, the approximation in level 2 which already contains a low frequency, is decomposed again into its lower frequency components, resulting in a signal with a low frequency and low amplitude, as shown in Figure 16. The detail 3, which contains a high frequency, has a similar profile to the original signal even though it has some noise left in it because, during the process, the approximation 2 is decomposed again into the low-frequency component and the high-frequency component, which makes the main echo signal is considered as high-frequency component and labelled as the detail.

### 5.7. THE ANALYSIS OF ECHO SIGNAL BY USING TIME-FREQUENCY REPRESENTATION

As discussed earlier, the deficiency of the conventional Fourier transform is the inability to observe the change of the frequency over time, because by using this method, all parameters about time will be missing. Moreover, this method becomes less effective if the measured signal is not stationary and has a characteristic that changes over time. The short time Fourier transform (STFT) method can actually overcome this problem, where the method works by dividing a signal into a few components that are assumed to be stationary [24]. Unlike the STFT method, the time-frequency representation by using Wavelet offers more benefits, where a better resolution either in time or frequency resolution can be obtained. This method is suitable to be applied to the echo signal which characteristics are changing over time when propagating into some mediums.

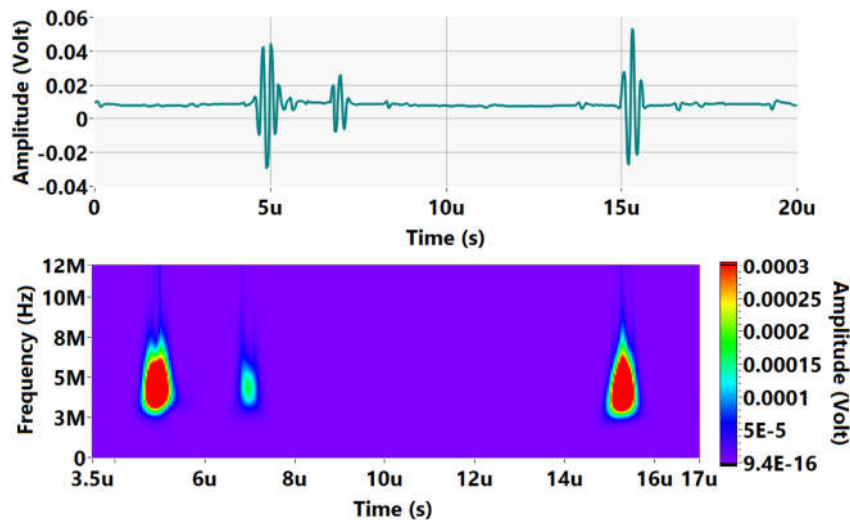


**Figure 19.** The echo signal in time domain (left) and the result of the echo signal in time-frequency domain (Scalogram)

Figure 19 shows the time representation of the echo signal of 4% saline solution (filtered by UWT) with the Scalogram as the output (lower figure), compared to the time domain of the echo signal (upper figure). From this result, the observation of the information and parameters of the echo signal

such as time, amplitude and the frequency of the signal can be performed easily, where  $S_1$  occurs at the time of 7 us, with the frequency around 3 to 6 MHz and the amplitude of around 0.0001 volts to 0.00025 volts. The  $S_0$  signal, which is at the time of 4 us, and the  $S_2$  signal which is at the time of 15 us can also be located easily, by observing the Scalogram result.

### 5.8. THE NORMALIZATION GRAPH OF RMS AND PEAK

In the previous research, Agus Indra Gunawan [1], had already built a calculation method to calculate the received intensity of the two-dimensional of the potential distribution of ultrasound. The calculation was done by transforming a 2D potential distribution of ultrasonic wave into a 2D plane wave k-space by using Fourier transform, thus the total intensity received at the transducer was calculated by summing all components of the potential distribution in real space. A similar method of calculation is also performed in this research, with the parameter of acrylic that is taken from the previous research [25], which measured the propagation of an ultrasonic guided wave in an acrylic plate. The comparison of the result between the calculation and the measurement (processed with Wavelet) is shown in Table 1, and the plotting of each result is shown in Figure 20. From Table 1, by comparing the result of the RMS and peak of all method with the result of the calculation shows that the error of the RMS value by using UWT method is the smallest among all. The 2% and 4% (RMS) of saline with the UWT method have a larger error (0.012771 and 0.012564 respectively) compared to the other value by using the same method. The percentage error of both values is 1.32257% and 1.34036% respectively. However, this deviation is acceptable since the error is less than 2%.

**Table 1.** The normalization value of RMS and peak (Wavelet, original, calculation)

% Saline	Calc.	No Wavelet				UWT				DWT			
		RMS	error %	Peak	error %	RMS	error %	Peak	error %	RMS	error %	Peak	error %
0	1	1	0	1	0	1	0	1	0	1	0	1	0
2	0.965618	0.919409	4.78543	0.925926	4.110528	0.952847	1.322573	0.979366	1.4237514	0.940316	2.620291	0.988684	2.388729
4	0.937358	0.916576	2.21708	0.878307	6.299728	0.924794	1.340363	0.905368	3.4127836	0.923567	1.471263	0.864324	7.791473
6	0.908786	0.869121	4.36461	0.84127	7.429252	0.912948	0.457974	0.867259	4.5695026	0.911659	0.316136	0.810117	10.85723
8	0.879911	0.857208	2.58015	0.809524	7.999332	0.881199	0.146378	0.839801	4.5584156	0.879937	0.002955	0.756995	13.96914
10	0.854373	0.799274	6.44906	0.804233	5.868631	0.848705	0.66341	0.76175	10.84105	0.847167	0.843426	0.803363	5.97046
Mean	0.924341	0.893598	3.39939	0.876543	5.284578	0.920082	0.655116	0.892257	4.1342505	0.917108	0.875678	0.870581	6.829506

The normalized peak-to-peak and RMS result of the measurement of the saline solutions by using UWT method is plotted in the graph. The result of the calculation and the original signal (without Wavelet) are also plotted as a comparison. The normalization is done by using the 0% of saline solution (pure water) as the reference. In the calculation, it is assumed that all parameters are constant. In Figure 20, the RMS value of the UWT method (red line) is the only parameter with the closest trend to the result of the calculation (blue line), and with the mean percentage error of 0.65512% that

is the smallest value among all. The small deviation of the saline solution with the weight percentage of 2% and 4% in the RMS graph (UWT) from the result of the calculation can be caused by many factors, even though a better signal processing like Wavelet transform has been performed. One of the factors is because, in the experiment, the trigger voltage sent to the transducer is small, that is only 10 Volts.

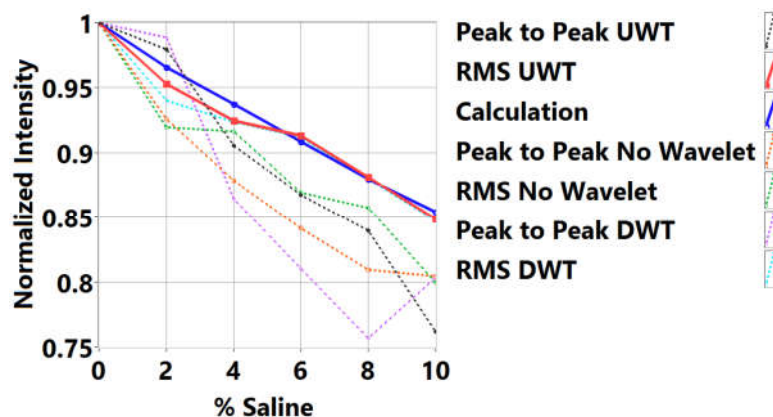


**Figure 20.** The comparison of normalized RMS and peak-to-peak graph (without Wavelet, with Wavelet and with calculation)

This makes the resulting echo signal is covered with noise which amplitude is almost at the same voltage as the received echo signal. If the voltage is raised, the noise may not affect the echo signal much because the amplitude of the echo signal will be larger. And also, in this research, the echo signal is directly acquired by the acquisition module, without any filtering component used. A better echo signal may be obtained if an appropriate hardware as a pre-filtering part before sending the signal to the acquisition module is applied. However, from the RMS result by using the UWT above, the Wavelet denoising method can perform an improvement in the echo signal in term of RMS value. As for the peak-to-peak detection, only the UWT method which is able produce a good trend, since the DWT method tends to change the profile of the original signal, as discussed in Section 5.1 earlier. Therefore, from this result, the Wavelet method has a capability to provide a better result in term of RMS value, compared to the original signal.

## 6. CONCLUSION

The Wavelet transform for enhancing the profile of the 3 MHz ultrasonic echo signal was performed. The enhancement includes the denoising process and the peak-to-peak detection. The output is the value of RMS and peak-to-peak which are applied as the basis data to develop a conversion curve. The analysis of the echo signal by using multiresolution and time-frequency analysis were also proposed.

The denoising process is performed by using the DWT and UWT method, the result shows that UWT provides a better output profile of the

echo signal, because UWT can remove the noise as well as maintaining the original profile of the echo signal, compared to the DWT method. The peak-to-peak detection by using Wavelet also provides more precision in detecting the peak and the valley of the signal, compared to the curve fitting method.

From the result of the normalization graph of peak-to-peak and RMS of saline solution with a different level of weight percentage, compared with the result of the calculation, the parameter of RMS with the UWT method has the closest trend to the result of the calculation, with the mean percentage error value of 0.65512%, which is the smallest among all parameters. The deviation is only located in the saline with 2% and 4% of weight percentage. One of the possible reasons is because, in the experiment, the trigger voltage sent to the transducer is pretty low (10 Volts), which makes the amplitude of the noise is at the same voltage as the original signal. For the next development of the research, a larger trigger voltage used in the system and a compatible pre-filtering hardware may lead to a better result of the echo signal. Based on the result of the normalization graph, the Undecimated Wavelet Transform (UWT) can be applied to enhance the profile of the 3 MHz ultrasonic echo signal, especially to calculate the RMS and peak-to-peak value. However, in terms of developing the conversion curve, only the RMS value which has the closest trend to the result of the calculation.

### Acknowledgements

A part of this study was financially supported by P3M (Research Center and Community Service) of PENS (Politeknik Elektronika Negeri Surabaya).

### REFERENCES

- [1] A. I. Gunawan, N. Hozumi, **Numerical Analysis of Ultrasound Propagation and Reflection Intensity for Biological Acoustic Impedance Microscope**, *Elsevier, Ultrasonics Journal*, Vol. 61, No. 4, pp. 102-110, 2015.
- [2] A. Nakano, T. Uemura, **Non-contact Observation of Cultured Cells by Acoustic Impedance Microscope**, *IEEE International Ultrasonic Symposium Proceedings*, pp. 1893 – 1896, 2008.
- [3] N. Hozumi, A. I. Gunawan, **Sound Field Analysis for Biological Acoustic Impedance Microscope for Its Precise Calibration**, *IEEE International Ultrasonics Symposium (IUS)*, pp. 1212 – 1215, 2013.
- [4] A. I. Gunawan, B. S. B. Dewantara, **Characterizing Acoustic Impedance of Several Saline Solutions Utilizing Range Finder Ultrasonic Sensor**, *IEEE International Electronics Symposium on Engineering Technology and Applications (IES-ETA)*, pp. 212 – 216, 2017.
- [5] A. I. Gunawan, Y. Saijo, **Acoustic Impedance Estimation Using Calibration Curve for Scanning Acoustic Impedance Microscope**, *International Conference on Knowledge Creation and Intelligent Computing (KCIC)*, pp. 240 – 245, 2016.

- [6] A. I. Gunawan, N. Hozumi, **Projection Mode Ultrasonic Microscopy for Cell-size Observation**, *IEEE International Ultrasonics Symposium (IUS)*, pp. 884 – 887, 2013.
- [7] N. Hozumi, A. Kimura, **Acoustic Impedance Micro-Imaging for Biological Tissue Using a Focused Acoustic Pulse With a Frequency Range up to 100 MHz**, *IEEE Ultrasonics Symposium*, Vol. 1, pp. 170 – 173, 2005.
- [8] N. Hozumi, S. Yoshida, **Observation of Rat Brain Tumor Model and Its Quantitative Analysis by Acoustic Impedance Microscopy**, *IEEE International Ultrasonics Symposium*, pp. 2372 – 2375, 2012.
- [9] N. Hozumi, A. Nakano, **Precise Calibration for Biological Acoustic Impedance Microscope**, *IEEE Ultrasonics Symposium Proceedings*, pp. 801 - 804, 2007.
- [10] A. Abbate, J. Koay, **Signal Detection and Noise Suppression Using a Wavelet Transform Signal Processor : Application to Ultrasonic Flaw Detection**, *IEEE Transactions on Ultrasonics, Ferroelectrics, and Frequency Control*, Vol. 44, pp. 14 – 26, 1997.
- [11] X. Zhu, J. Kim, **Application of Analytic Wavelet Transform to Analysis of Highly Impulsive Noises**, *Elsevier, Journal of Sound and Vibration*, Vol. 294, No. 4, pp. 841 – 855, 2006.
- [12] N. Akshay, N. A. V. Jonnabhotta, **ECG Noise Removal and QRS Complex Detection Using DWT**, *IEEE International Conference on Electronics and Information Engineering*, Vol. 2, No. 2, pp. V2-438 – V2-442, 2010.
- [13] V. N. P. Raj, T. Venkateswarlu, **ECG Signal Denoising Using Undecimated Wavelet Transform**, *IEEE 3rd International Conference on Electronics Computer Technology*, Vol. 3, pp. 94 – 98, 2011.
- [14] Z. Yu, C. Zhao, **Application of the Wavelet Transform in Ultrasonic Echo Signal Processing**, *IEEE Second International Workshop on Computer Science and Engineering*, Vol. 1, pp. 576 – 579, 2009.
- [15] Herlinawati, U. Murdika, **Ultrasonic Signal Denoising Based on Wavelet Haar Decomposition Level**, *IEEE 3rd International Conference on Information Technology, Computer and Electrical Engineering (ICITACEE)*, pp. 89 – 94, 2016.
- [16] J. L. S. Emeterio, M. A. Rodriguez-Hernandez, **Wavelet Denoising of Ultrasonic A-Scans for Detection of Weak Signals**, *IEEE 19th International Conference on Systems, Signals and Image Processing (IWSSIP)*, pp. 48 – 51, 2012.
- [17] M. K. A. Hassan, K. Nagamune, **Wavelet Decomposition Processing Method : Cortical Bone Thickness Measurement Using Ultrasound Sensor**, *IEEE International Conference on Systems, Man, and Cybernetics (SMC)*, pp. 3941 – 3945, 2014.
- [18] K. Elmansouri, R. Latif, **Efficient Fetal Heart Rate Extraction Using Undecimated Wavelet Transform**, *IEEE Second World Conference on Complex Systems (WCCS)*, pp. 696 – 701, 2014.

- [19] M. S. Fathillah, R. Jaafar, **Interictal Epileptic Discharge EEG Detection Based on Wavelet and Multiresolution Analysis**, *IEEE International Conference on System Engineering and Technology (ICSET)*, pp. 140 – 144, 2017.
- [20] National Instrument Cooperation, **Wavelet and Filter Bank Design Toolkit Reference Manual**, *National Instrument*, Ed. June, 2008.
- [21] A. M. Gaouda, M. M. A. Salama, **Power Quality Detection and Classification Using Wavelet-Multiresolution Signal Decomposition**, *IEEE Transactions on Power Delivery*, Vol. 14, No. 4, pp. 1469 – 1476, 1999.
- [22] C. Tepe, N. Senyer, **Improving R-peak Detection in ECG Based on Polynomial Curve Fitting**, *IEEE International Conference on Application of Information and Communication Technologies*, pp. 1 – 4, 2009.
- [23] U. Zaka, B. A. Baloch, **Detection of Peaks of ECG Using Wavelet Transform**, *IEEE National Software Engineering Conference*, pp. 43 – 47, 2014.
- [24] A. A. Jaber, R. Bicker, **A Simulation of Non-stationary Signal Analysis Using Wavelet Transform Based on LabVIEW and Matlab**, *IEEE European Modelling Symposium*, pp. 138 – 144, 2014.
- [25] K. I. Lee, B. K. Choi, **Propagation of Ultrasonic Guided Waves in an Acrylic Plate as a Cortical-bone-mimicking Phantom**, *Journal of the Korean Physical Society*, Vol. 65, pp.1858 – 1862, 2014.